CIMA meeting: Event classification

K. Brzeziński

1. Types of events

Coincidence sorting was performed on the processed list-mode singles data. The coincidences were classified as ring-ring and ring-probe. Coincidences involving one detection in the ring and multiple detected interactions in the probe were estimated separately. For each type, the contribution of true coincidences was estimated as well as that of accidental coincidences (randoms) which degrade image. The amount of coincidence events that contain a scattered photon, another source of image degradation, were also estimated. The effect of the coincidence timing window (CTW) and the low-energy threshold (LET) in the Si detector on the various event types was investigated.

1.1. True coincidences

A true coincidence is the detection of two photons, originating from the same annihilation event, within the CTW. These are the events that provide information about the activity distribution being imaged. Figure 1 shows a schematic diagram of such a coincidence event.

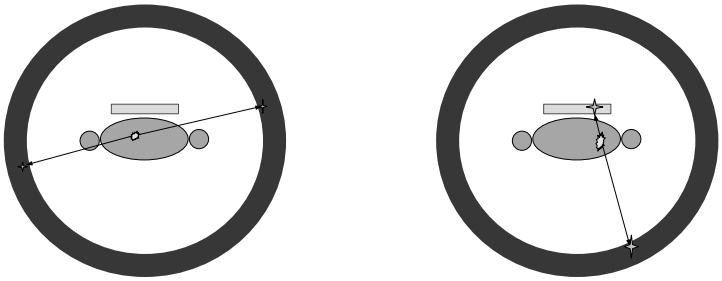

(a) (b)

Figure 1. Schematic diagram of a true a) ring-ring coincidence and b) probe-ring coincidence. The two detected photons originate from the same annihilation event.

1.2. Randoms

A random coincidence is the detection of two photons, originating from different annihilation events, within the CTW. These events provide no information about the activity distribution being imaged and can even be interpreted as originating outside of the FOV, if some shielding is not applied. Figure 2 shows a schematic diagram of such a coincidence event.

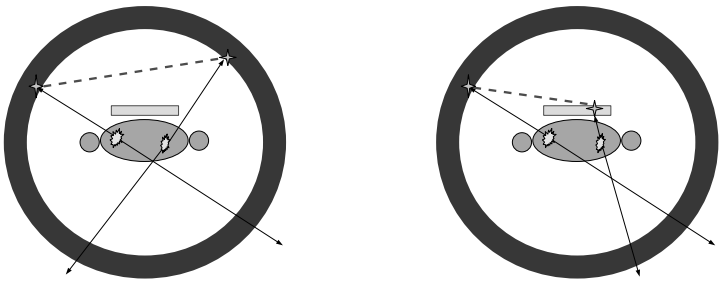

(a) (b)

Figure 2. Schematic diagram of a random a) ring-ring coincidence and b) probe-ring coincidence. The two detected photons originate from two separate annihilation events.

1.3. Multiple Coincidences

Probe-ring coincidences may involve multiple detections of the same photon in the probe. Due to time uncertainty in the Si detectors it is difficult to determine the order of the probe interactions, which is essential if the event is to be used in reconstruction. For this reason this type of event is not used for reconstruction in the work. Nevertheless, it is usefull to measure its contribution. Figure 3 shows a schematic diagram of such a coincidence event.

1.4. Phantom-Scattered Events

Before reaching the detectors, many annihilation photons scatter in the object being imaged. Due to the change in trajectory the photons undergo, these events reduce the resolution information provided. Figure 4 shows a schematic diagram of such a coincidence event.

1.5. Undetected Scatter in Si Detectors

Before being detected, some annihilation photons may undergo scatter in the sensitive detector material but, because they deposit an amount of energy inferior to the LED in that detector, generate no signal from it. Such is the case of the well-know phenomenon of inter-crystal scatter where a photon interacts in one scintillator detector, depositing a small amount of energy, but is absorbed in its neighboring one. In the PET-probe

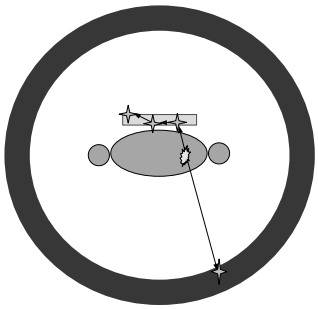

Figure 3. Schematic diagram of a multiple coincidence. The two detections in the probe originate from the same photon.

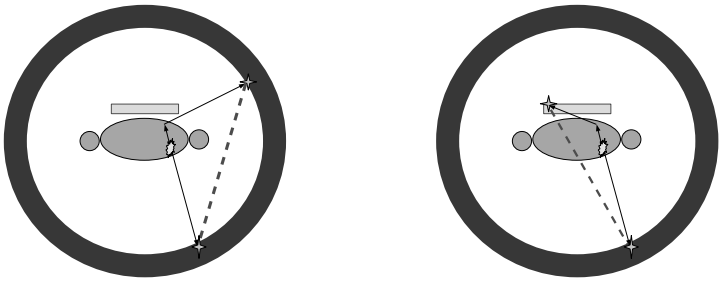

(a) (b)

Figure 4. Schematic diagram of a phantom-scattered a) ring-ring coincidence and b) probe-ring coincidence. Here, one of the photons undergoes scatter in the phantom before being detected.

system, there is the additional effect of undetected scatter in the probe. In this study we consider only those photons scattered in the probe's sensitive material that deposit an energy lower than the LED in the Si. Scattering may also occur in parts of the probe's structure and electronics. As in the case of object scatter, the change in trajectory these photons undergo, causes a reduction of the resolution information they carry. Figure 5 shows a schematic diagram of such a coincidence event.

2. Effect of Coincidence Timing Window

The choice of the CTW in coincidence sorting affects the amount of certain types of events present in the coincidence data. True coincidences, randoms and multiple coincidences in the probe are the events directly affected by this parameter. Activity levels also have an effect on the rate of these event types and therefore should be considered when measuring the contribution due to these events. To measure the effect of the CTW on the amount trues, randoms, and multiple scatters in the coincidence

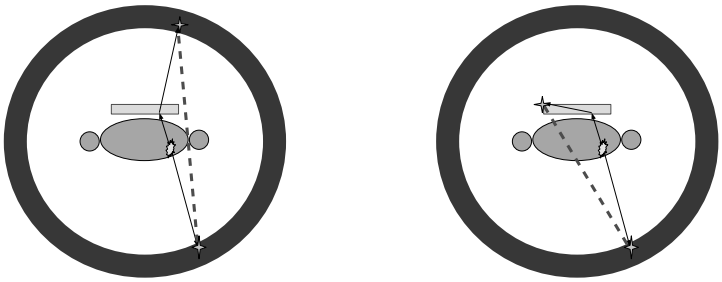

(a) (b)

Figure 5. Schematic diagram of a) inter-crystal scatter, were the two interactions from the single photon occur in different crystals, and b) a probe-scattered event.

data simulations were performed using the NEMA PET Scatter Phantom. This phantom, designed to standardize the measurement of count rate performance of PET devices in the presence of scatter, consists of an axially centered polyethylene cylinder, 70 cm in length and 20.3 cm in diameter. The phantom contains a line source, 80 cm long, axially centered at a radial offset of 4.5 cm. We perform our simulations at three different activities: 1 mCi, 5 mCi and 10 mCi. The middle value represents a typical activity given to a patient during an FDG study. In order to observe the effects of the CTW, coincidence sorting was performed using CTWs of 4.5, 10, 15 and 20 ns, the limitting values chosen to be double the time resolution of the LSO and Si detectors respectively. The probe was centred at 120 mm from the center of the FOV, its surface being 8.5 mm away from the phantom surface and 65 mm away from the line source. A block difference of 14 was imposed to reduce random coincidences by disallowing ant LOR that does not pass through a 70 cm bore.

2.1. True Coincidences

Figure 6 demonstrates how the true coincidence rate varies with the CTW and activity for a 1 s simulation. In figure 6 a) we see that as the CTW is increased there is a reduction of ring-ring sensitivity to true events. At 1 mCi this trend is very small but increases with activity and becomes significant at 10 mCi, falling to almost half at 20 ns CTW compared to the value at 4.5 ns. Figure 6 b) demonstrates that the probe-ring true coincidence rate peaks when using the 10 ns CTW. Again this trend is most notable for the higher activities and small for the 1 mCi case.

2.2. Randoms

Figure 7 demonstrates how the randoms coincidence rate varies with the CTW and activity, for a 1 s simulation. Figure 7 a) and b) shows how the ring-ring probe-ring randoms rates increase with the CTW.

Figure 8 shows the amount of random coincidences as a fraction of the total, that is the random fraction.

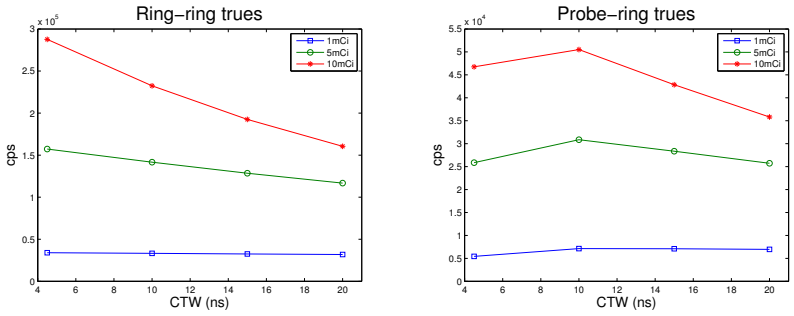

(a) (b)

Figure 6. Plots of the true coincidence rate for different CTWs and activities for a) ring-ring and b) probe-ring events.

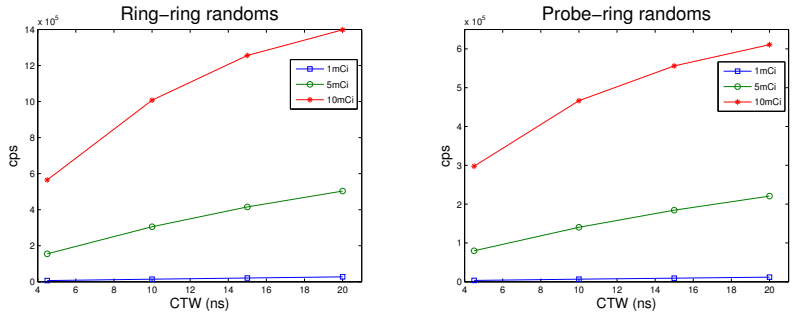

(a) (b)

Figure 7. Plots of the random coincidence rate for different CTWs and activities for a) ring-ring and b) probe-ring events.

2.3. Multiple Coincidences

Figure 9 shows a plot of the rate of probe-ring events where photon detected in the probe produces signal in various Si pixels. It can be seen how this quantity increases with increased CTW.

3. Effect of Low Energy Threshold in the Probe

A 10 ns CTW was used. Same setup as above.

3.1. Sensitivity

Figure 10 shows the total number of ring-ring and probe-ring coincidence events as a function of LED in the Si pixels.

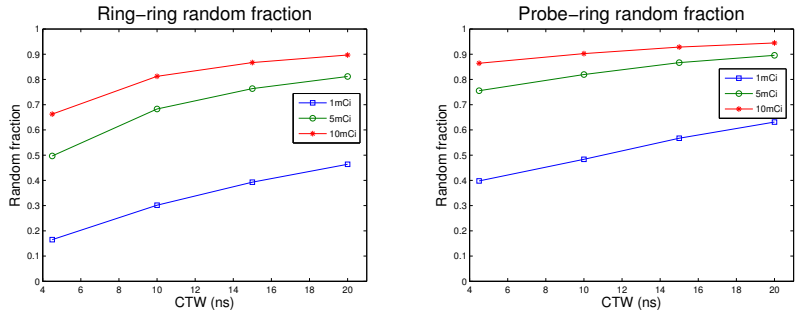

(a) (b)

Figure 8. Plots of the random fractions for different CTWs and activities for a) ring-ring and b) probe-ring events.

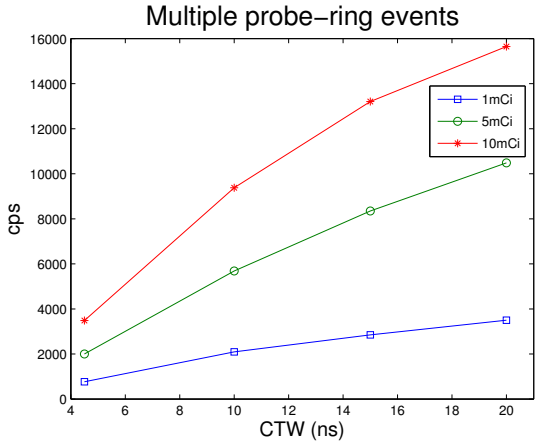

Figure 9. Plot of the probe-ring coincidence rate, with multiple coincidences in the probe, for different CTWs and activities.

3.2. Phantom Scattered Events

Figure 11 shows the phantom-scattered fraction for the ring-ring and probe-ring coincidence events as a function of LED.

3.3. Undetected Scatter in Si Detectors

Figure 12 shows the fraction of ring-ring and probe-ring coincidence events that underwent undetected scatter in the Si detectors, as a function of Si LED.

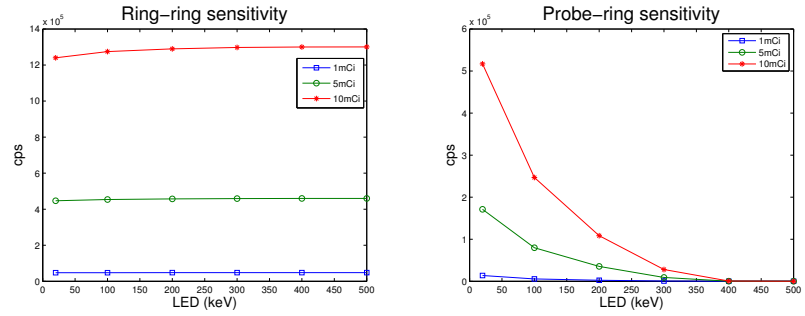

(a) (b)

Figure 10. Plots of the coincidence rates for different LEDs and activities for a) ring-ring and b) probe-ring events.

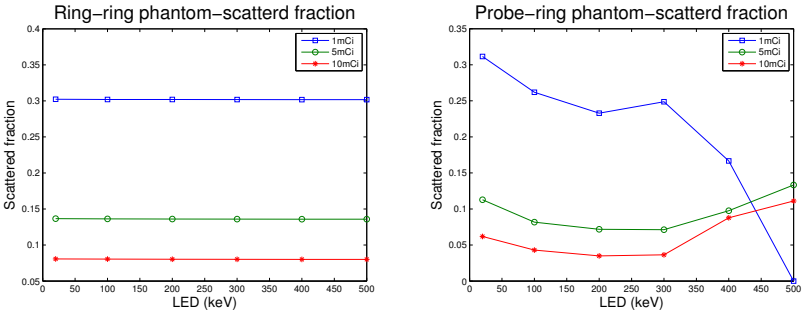

(a) (b)

Figure 11. Plots of the phantom-scattered fraction for different LEDs and activities for a) ring-ring and b) probe-ring events.

3.4. Total Scattered Fraction

Figure 13 shows the total scattered-fraction, due to undetected scatter in the probe and scatter in the phantom, as a function of Si LED.

3.5. Multiple Coincidences

Figure 14 shows a plot of the rate of probe-ring events where the photon detected in the probe produces signal in various Si pixels, as a function of LED in the Si pixels.

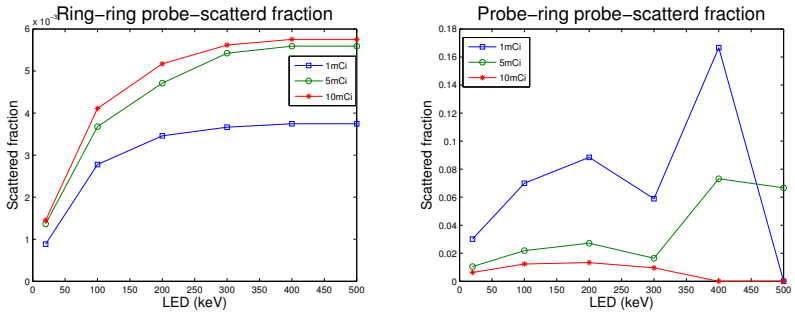

(a) (b)

Figure 12. Plots of the probe-scattered fraction for different LEDs and activities for a) ring-ring and b) probe-ring events.

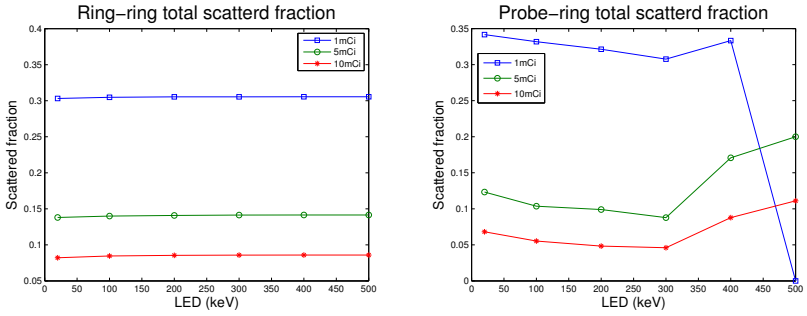

(a) (b)

Figure 13. Plots of the total scattered fraction, including that due to scatter in the probe, for different LEDs and activities for a) ring-ring and b) probe-ring events.

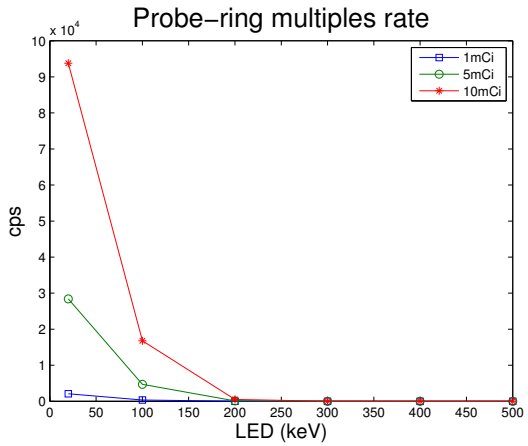

Figure 14. Plot of the probe-ring coincidence rate, with multiple coincidences in the probe, for different LEDs and activities.